PPS www.rsc.org/pps

Ship-in-a-bottle synthesis of 2,4,6-triphenylthiapyrylium cations encapsulated in zeolites Y and beta: a novel robust photocatalyst

Mercedes Alvaro, Esther Carbonell, Hermenegildo Garcia,* Cristina Lamaza and Manoj Narayana Pillai

Instituto de Tecnología Química and Departamento de Química, Universidad Politécnica de Valencia, 46022 Valencia, Spain. E-mail: hgarcia@qim.upv.es

Received 3rd September 2003, Accepted 28th October 2003
First published as an Advance Article on the web 13th November 2003

The 2,4,6-triphenylthiapyrylium ion has been obtained imprisoned inside the supercages of the tridirectional, large pore zeolites Y and beta *via* ship-in-a-bottle synthesis from chalcone and acetophenone in the presence of hydrogen sulfide. The resulting solids are efficient and robust photocatalysts that are able to degrade phenol and aniline in water with a higher efficiency than the P-25 TiO_2 standard. Preliminary tests have shown that these encapsulated dye materials are also efficient photocatalysts for the oxidative degradation of malodorous sulfur-containing molecules.

Introduction

Among the sensitizers that have been used in photoinduced electron transfer (PET), the 2,4,6-triphenylpyrylium cation (TP^+) has a number of advantageous characteristics:[1] (i) high oxidation potentials (>2 V *vs*. SCE) in both the singlet and triplet excited states;[1] (ii) long wavelength absorption bands (370 and 420 nm);[1] (iii) the inability to generate singlet oxygen; (iv) the net Coulombic interaction does not change after PET.

Some time ago, we prepared TP^+ inside zeolites Y and beta, and showed that the resulting solids (TP@Y and TP@β) can be used as heterogeneous sensitizers in photocatalytic processes.[2,3] Incorporation of TP^+ in the zeolite supercages modifies the molecular properties of the cationic heterocycle in a favorable way. In particular, when encapsulated in zeolite Y, TP^+ does not undergo hydrolysis at room temperature and photolysis of aqueous solutions of TP@Y generates hydroxyl radicals.[4] The above characteristics of TP@Y (which are different from those of soluble TP^+ salts, which undergo hydrolysis and heterocycle ring opening in water) enable TP@Y to be used as an organic photocatalyst for the mineralization of water-borne organic pollutants with sunlight. For this application, TP@Y can exhibit higher efficiency than the P-25 TiO_2 standard.[4,5] The search for more efficient photocatalysts with increased durability and service lifetime is an ongoing task that could eventually lead to the introduction of photocatalytic techniques as a viable treatment for waste water remediation.[6]

In this paper, we report the preparation and screening of the photocatalytic activity of 2,4,6-triphenylthiapyrylium ($TPTP^+$) embedded inside the cages of zeolites Y and beta. The novel TPTP@zeolite photocatalysts are more active and robust than the previous TP^+ analogs. Our photocatalytic results seem to mirror the relatively higher thermal stability of thiapyrylium cations compared to pyrylium cations.[7] This stability derives from the lower electronegativity of S compared to O, which leads to better charge delocalization and a greater degree of aromaticity for thiapyrylium with respect to pyrylium,[7] while the photochemical properties of both moieties are similar.[8,9]

Results and discussion

The simplest strategy to prepare $TPTP^+$ encapsulated within zeolites is to exchange the heteroatom in TP@Y, the synthesis of which is already established, using HS^- as a nucleophile (eqn. 1).

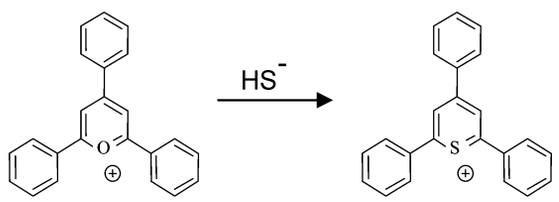

(1)

This reaction works well in solution and gives quantitative yields.[7] However, all our attempts to transform TP^+ into $TPTP^+$ by stirring a suspension of TP@Y in 0.1 M aqueous HS^- at various temperatures were unsuccessful. This failure was not totally unexpected, since when TP^+ is encapsulated in zeolite, it is unaffected by water, whereas it undergoes fast hydrolytic ring opening in solution.[10] Steric restrictions imposed by the rigid zeolite walls on the conformational movements required for nucleophilic attack have been proposed to explain the stability of encapsulated TP@Y.[10]

On the other hand, given the large molecular size of $TPTP^+$ (similar to TP^+), its encapsulation inside the supercages of the zeolites cannot be accomplished by ion exchange of preformed $TPTP^+$ from the exterior to the interior of the pores. Therefore, the only viable strategy is to devise a ship-in-a-bottle synthesis in which small precursors that can diffuse through the pores form the target molecule inside the zeolite cavities. The ship-in-a-bottle methodology to entrap large species within the cavities of zeolite Y was initially devised by Schulz-Ekloff *et al*. for the preparation of metallic complexes,[11] and the term was later coined by Herron *et al*.[12] and Lundsford *et al*.[13]

The synthesis of zeolite-encapsulated $TPTP^+$ was accomplished by reacting two equivalents of chalcone and one of acetophenone in the presence of zeolite suspended in H_2S-saturated cyclohexane (Scheme 1).

Since the synthesis of $TPTP^+$ is catalyzed by acids, we used the H^+ form of the zeolites Y (Si/Al = 17, surface area 540 $m^2\ g^{-1}$) and beta (Si/Al = 13, surface area 470 $m^2\ g^{-1}$). The suspension was magnetically stirred at reflux temperature for 72 h. Then, the resulting yellow solid was subjected to exhaustive solid–liquid extraction to remove by-products and excess starting materials. Fig. 1 shows a molecular model of $TPTP^+$ entrapped within a zeolite Y supercavity.

It is important not only to demonstrate the formation of $TPTP^+$ but also the absence of TP^+ impurities that could be formed concurrently. Formation of $TPTP^+$ inside the solid was assessed by diffuse reflectance UV-Vis (DR-UV) and FT-IR spectroscopy. Fig. 2 shows the characteristic $TPTP^+$ absorption

DOI: 10.1039/b310627f

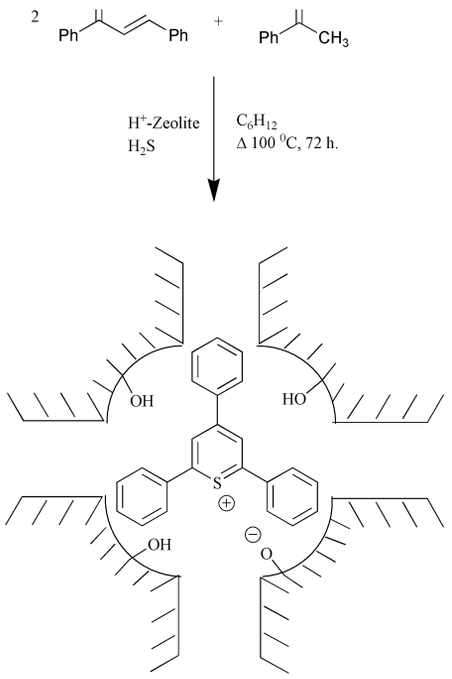

Scheme 1 Ship-in-a-bottle synthesis of 2,4,6-triphenylthiopyrylium ion encapsulated in zeolite.

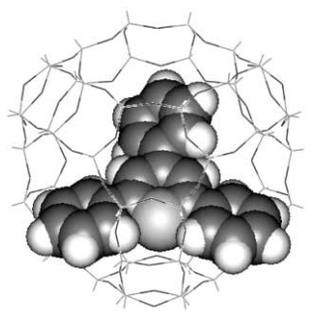

Fig. 1 Molecular modeling representation of $TPTP^+$ immobilized inside a supercage of ideal all-silica zeolite Y.

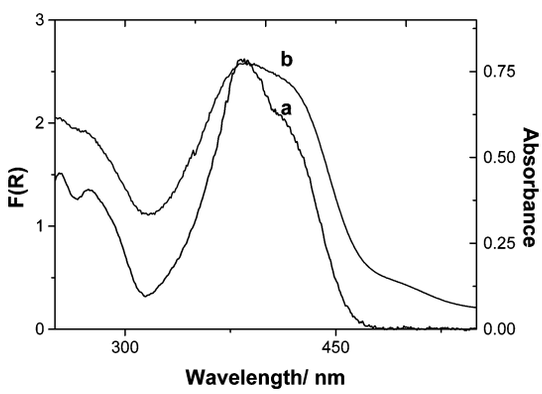

Fig. 2 (a) UV-Vis spectrum of $TPTP^+ClO_4^-$ in CH_2Cl_2 (absorbance). (b) DR-UV spectrum of TPTP@Y (plotted as the Kubelka–Munk function of the reflectance).

band in the visible region (λ_{max} 380 nm, shoulder at 420 nm). Interestingly, the absorbance minimum at 320 nm in the DR-UV spectra was found an indicator to confirm the absence of adventitious by-products. Aromatic ketones have an absorption maximum around 300 nm and a valley in the optical spectrum of the solid demonstrates their absence. Other samples where significant amounts of impurities are present, as evidenced by FT-IR, do not exhibit this valley at 310 nm.

IR spectroscopy was a very useful technique for the structural characterization of the TPTP@Y samples, especially for demonstrating that the samples were free from TP^+. Since TP^+ is formed by a similar reaction procedure, except that no H_2S is involved, it is necessary to address the possibility of formation of variable amounts of TP^+ during the synthesis of $TPTP^+$. This issue is particularly important given that the routes to formation of TP^+ and $TPTP^+$ have common intermediates. The DR-UV spectra of TP^+ and $TPTP^+$ are so similar that Fig. 2 cannot conclusively rule out the presence of some TP^+ as an impurity. In contrast, TP^+ exhibits a characteristic strong $C{=}O^+$ vibration at 1623 cm^{-1} in the IR that should be absent in $TPTP^+$. Fig. 3 shows that only a weak band is observed at 1623 cm^{-1} in the IR spectra of well-prepared TPTP@zeolites. Quantitative estimation based on the relative intensity of the 1623 cm^{-1} band indicates that the upper limit of TP^+ impurities in the TPTP@zeolite is 1 in 100 zeolite Y supercages (see below for quantification of the $TPTP^+$ loading). On the other hand, the IR spectrum for TPTP@zeolites is remarkably similar to that of $TPTP^+ClO_4^-$ (note the presence of a weak band at ~1620 cm^{-1} for the authentic $TPTP^+ClO_4^-$ sample also). It is worth pointing out that in some experiments, variable amounts of TP^+ and $TPTP^+$ were concurrently formed inside the zeolite, as evidenced by the simultaneous observation of bands characteristic of $TPTP^+$ and TP^+ in the IR spectra of the samples. The proportion of adventitious TP^+ is particularly high when the ship-in-a-bottle synthesis is carried out at lower temperatures or when the reaction medium and zeolite are not constantly purged with a H_2S stream.

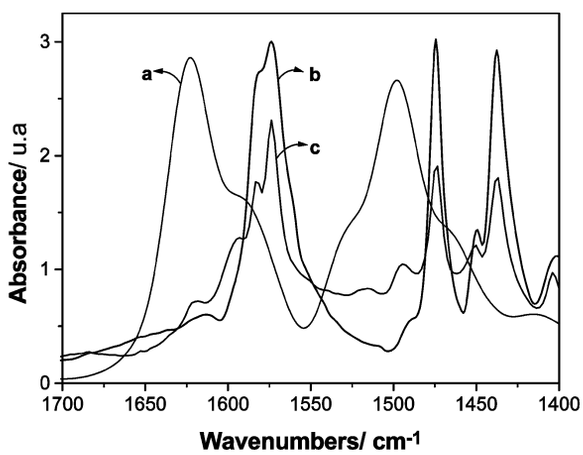

Fig. 3 Fingerprint region of the FT-IR spectra of $TP^+BF_4^-$ (a), $TPTP^+ClO_4^-$ (b) and TPTP@Y (c). The spectrum of TPTP@Y was recorded at room temperature after outgassing at 200 °C and 10^{-2} Pa to remove co-adsorbed water.

The location of $TPTP^+$ inside the zeolite particles was inferred from the decrease in the intensity in the IR spectra of the zeolite acidic OH stretching band corresponding to internal Brønsted sites (3650 cm^{-1}) that become partially replaced by $TPTP^+$. As the formation of $TPTP^+$ progresses, an equivalent amount of the acidic bridging ≡Si–(OH)–Al≡ silanol groups should be replaced by $TPTP^+$, leading to the decrease in the population of these bridging OH groups observed in the IR spectra (Scheme 1 shows $TPTP^+$ compensates for a negative ≡Si–O–Al^-≡ aluminium atom). The loading of $TPTP^+$ was determined by chemical analysis (5.85% C and 0.44% S) for typical TPTP@Y samples and corresponds roughly to an average occupancy of one $TPTP^+$ for every 3 supercages in zeolite Y. In the case of TPTP@β, the combustion analysis (3.19% C and 0.21% S) corresponds to an average of one $TPTP^+$ for every 9 channel crossings. For comparison, the carbon contents of TP@Y and TP@β used in this work to establish the relative photoactivity of thiopyrylium samples are 3.91 (one TP^+ for every 4 supercages) and 3.31% (one TP^+ for every 8 channel crossings), respectively. Thus, the loadings of $TPTP^+$ and TP^+ for each zeolite are comparable.

Photophysical properties

The utility of a solid as a photocatalyst depends to a large extent on the photophysical properties of the material. Characterization of the excited states generated upon light absorption can be achieved by combining information from emission spectroscopy and laser flash photolysis. Fig. 4 shows the emission spectrum recorded for TPTP@Y upon excitation at absorption maximum (420 nm). What is remarkable in this spectrum is the broadness of the emission band. Comparing the spectrum for TPTP@Y with the reported fluorescence (λ_{max} 470 nm) and low temperature phosphorescence spectra (λ_{max} 550 nm) of $TPTP^+BF_4^-$ in acetonitrile,[9] it can be concluded that the emission of the solid encompasses both fluorescence and room temperature phosphorescence. In contrast the ClO_4^- salt of $TPTP^+$ does not emit detectable phosphorescence at room temperature. This phenomenon has also been observed for TP@Y [14,15] and reflects the favorable intersystem crossing, leading to a high triplet population as well as enhancement of the radiation deactivation pathways. It has been suggested that immobilization and conformational restrictions imposed by the rigid framework on entrapped TP^+ favor emission and triplet generation by disfavoring radiationless deactivation pathways arising from thermal relaxation of the singlet excited state.

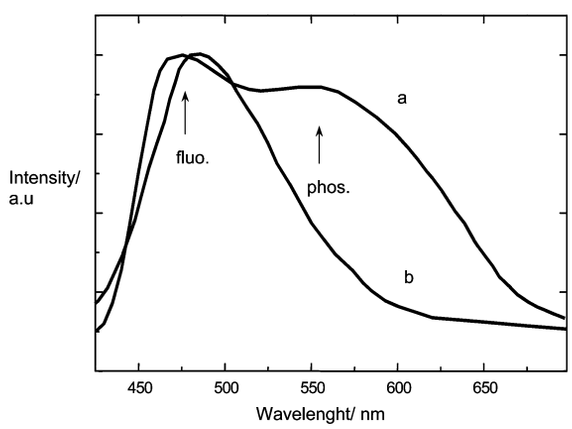

Fig. 4 Room temperature emission spectra of TPTP@Y (a) and $TPTP^+ClO_4^-$ in acetronitrile (b) upon excitation at 420 nm. The fluorescence and phosphorescence maxima are marked with arrows.

The coincidence of the maxima in the absorption and emission (fluorescence and phosphorescence) spectra, together with the electrochemical measurements (see below), suggest that the energy of the singlet and triplet excited states of $TPTP^+$ (E_S = 66 kcal mol^{-1}, E_T = 52 kcal mol^{-1}) are not changed upon encapsulation.

Laser flash photolysis of TPTP@Y also shows similarities with the TP@Y sample. Fig. 5 shows the transient spectrum recorded for TPTP@Y upon 355 nm laser excitation, the absorption being comparable with those reported for the triplet excitation states of other salts of $TPTP^+$.[9] In agreement with this, the signal is quenched by oxygen (Fig. 5, inset). It is remarkable that the triplet decay is not complete after hundreds of milliseconds. The enhancement of the triplet lifetime of $TPTP^+$ upon encapsulation is attributed to the restriction of conformational freedom which occurs upon entrapment of the ion in the confined space of the zeolite cage,[15] thus disfavoring radiationless deactivation pathways. This long triplet lifetime is an advantage for the application of this solid as a photocatalyst since longer lifetimes give a greater opportunity for dynamic quenching by allowing the substrate sufficient time to diffuse into the structure and react with the excited state.

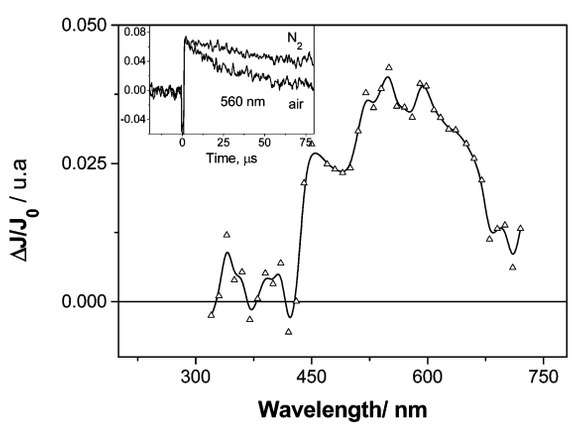

Fig. 5 Transient absorption spectrum recorded 15 μs after 308 nm laser excitation of a N_2-purged sample of TPTP@β. The inset shows the decay monitored at 560 nm.

Photocatalytic study of TPTP@zeolite

Even though encapsulation of TP^+ dramatically increases its stability as compared to solution, there should still be room for further improvements in its photocatalytic activity. Previous reports in the literature show that the photosensitizing activity of thiapyrylium heterocycles is higher than the pyrylium analogs.[8,9,16] Thus, based on the results for non-encapsulated dyes in solution we anticipated that the behavior of $TPTP^+$ zeolite would be similar to that of TP@Y, but with enhanced photochemical stability and activity. As test reactions, we selected the photocatalytic degradation of aqueous solutions of phenol and aniline in the presence and absence of H_2O_2.[17] H_2O_2 is a convenient source of hydroxyl radicals. The photochemical degradation of phenol has been proposed as a basis for comparing the photocatalytic activity of different TiO_2 solids,[18] while photocatalytic degradation of anilines using zeolite-encapsulated $Ru(bpy)_3^{2+}$ and the analogous iron complex has been studied recently.[17,19,20]

There are two important parameters to be considered in a photocatalytic reaction. The first one is the initial photocatalytic activity (v_0), obtained from the slope of the substrate disappearance profile at $t = 0$. This should give a measure of the photocatalytic activity [phenol degradation (%) per min] of the fresh zeolite samples. A plot of v_0 *versus* the amount of photocatalyst used for a series of runs in which the latter is varied for a constant concentration of pollutant serves to adequately compare sample activity (see Fig. 7).[18] The second parameter is the residual substrate concentration at the final reaction time. Obviously, the actual photocatalytic activity will depend on the light intensity and photoreactor design, but the relative order of the photocatalysts should remain independent of the experimental set-up.

As a representative example, Fig. 6 shows the percentage of phenol disappearance in aqueous solution in the presence

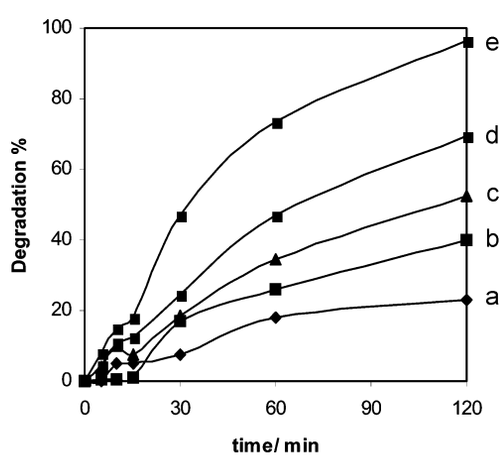

Fig. 6 Percentage of photocatalytic phenol degradation upon irradiation of 20 ml of a 40 ppm aqueous solution in the presence of 30 mg of various photocatalysts: (a) TP@Y; (b) TP@β; (c) TiO_2; (d) TPTP@Y; (e) TPTP@β.

of 30 mg of a series of photocatalysts. Our study screened different amounts of photocatalyst in the range 15–100 mg, keeping constant the concentration (40 ppm) and the volume (20 ml) of the phenol solution. TiO_2 (P-25 Degussa standard, surface area 30 m^2 g^{-1}) was also included in the study. In all cases, varying amounts of hydroquinone and quinone were observed as degradation products. As can be seen in Fig. 6, $TPTP^+$ encapsulated in either zeolites Y or beta exhibit higher v_0 values than the TP^+ analogs and even P-25, the photocatalytic activity of the catalysts follows the order TPTP@β > TPTP@Y > P-25 > TP@β > TP@Y. Exactly the same order of initial photocatalytic activity, but with different initial rates, is obtained when other runs with varying amounts of photocatalyst were performed (Fig. 7). Moreover, the final percentage of degradation also follows the same order as the initial activity, given a minimum turnover number for the phenol/$TPTP^+$ ratio of about 30. Irradiation in the presence of 10^{-3} M H_2O_2 increases the initial phenol degradation rate by a factor of 4 when TPTP@β is the photocatalyst.

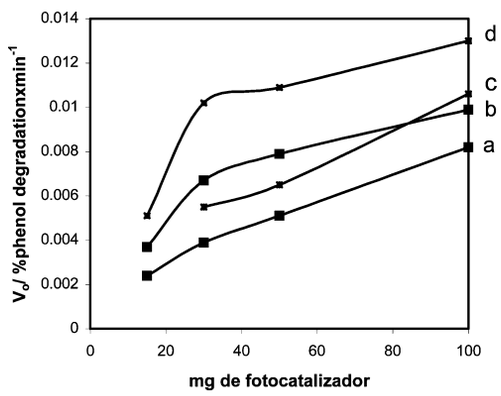

Fig. 7 Influence of the amount of photocatalyst on the initial degradation rate [v_0, phenol degradation (%) per min]: (a) TP@β; (b)TPTP@Y; (c) TiO_2; (d) TPTP@β. From these plots, 30 mg was selected as the appropriate amount of photocatalyst to use for the photocatalytic studies.

Parallel results were obtained for the photocatalytic degradation of aniline (Fig. 8). As expected,[19] addition of H_2O_2 significantly increases the v_0 for phenol and aniline degradation, although its presence is not necessary. In fact, iodimetric titration established that photolysis of TPTP@Y in distilled water generates a stationary 6×10^{-3} M concentration of H_2O_2. The DR-UV spectrum of the TPTP@β after the photocatalytic degradation of phenol shows that the $TPTP^+$ ion remains unaffected by the reaction. The order of the photoactivity of the catalysts is not determined by sensitizer loading in the zeolite, since TPTP@β and TP@β have similar loadings that are lower than those of the less active zeolite Y samples. In addition, preliminary tests have shown that TPTP@β is also an efficient photocatalyst for the oxidative degradation malodorous sulfur-containing molecules.

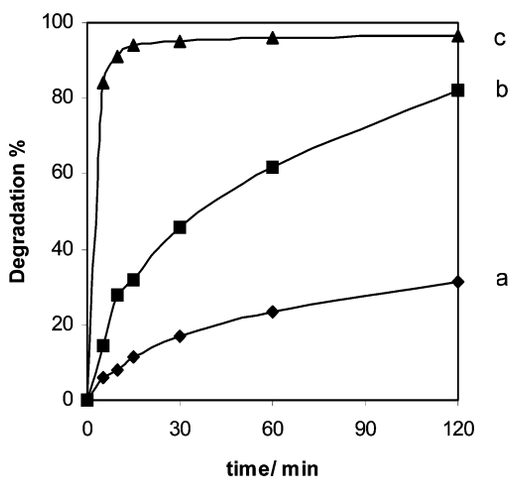

Fig. 8 Percentage of photocatalytic aniline degradation upon irradiation of 20 ml of a 40 ppm aqueous solution in the presence of 30 mg of various photocatalysts: (a) TP@Y; (b) TPTP@Y; (c) TPTP@β.

In order to understand the higher photocatalytic activity of $TPTP^+$ with respect to TP^+, we assume that the fraction of light absorbed for the different dye-containing photocatalysts is similar, since the dye loading of the samples is close and the absorption coefficients of TP^+ and $TPTP^+$ in solution are also similar. Therefore, the difference must be due to an intrinsic property of the dyes. Thus, the reduction potentials of TP@Y and TPTP@Y were measured by cyclic voltammetry, giving −0.260 and −0.240 V *vs.* SCE, respectively. These reduction potentials are in very good agreement with those reported for TP^+ and $TPTP^+$ in solution[16] and indicate that $TPTP^+$ is easier to reduce than TP^+. Taking these reduction potential values into account, as well as the singlet energy from the absorption spectrum, and considering the Rehm–Weller equation,[21] it can be proposed that the higher photocatalytic activity of TPTP@zeolite derives from the higher electron-abstracting ability of $TPTP^+$ (about 2 Kcal mol^{-1}) as compared to TP@zeolite. This conclusion parallels that previously drawn by Saeva and Ollin for the same dyes in solution and is based on the measured reduction potential of the dyes encapsulated within zeolites.[16] However, since higher exothermicity for a favorable photoinduced electron transfer may not lead to a higher photoactivity, other factors may contribute to enhance the photodegradation efficiency. In this regard, an alternative explanation for the higher intrinsic efficiency of photodegradation for TPTP@zeolite compared to TP@zeolite could be the difference in the lifetimes of the corresponding singlet and excited states of TP^+ and $TPTP^+$.

The photostability of TPTP@Y was checked by reusing it for a second run under the same experimental conditions. The photoactivity in the second run was found to be essentially the same as for the fresh sample, and diffuse reflectance UV-Vis spectroscopy showed that no bleaching of $TPTP^+$ had occurred after the two consecutive irradiations.

In summary, we have described in this paper the successful synthesis of $TPTP^+$ encapsulated in zeolites Y and beta. The photocatalytic performance of TPTP@β largely exceeds that of the oxygenated analog, TP^+, encapsulated in zeolites and the P-25 TiO_2 standard. This further improvement in the photocatalytic activity of encapsulated dyes brings the prospect of their application for photocatalytic degradation of contaminants in waste water.

Experimental

Preparation and characterization of the zeolite-encapsulated photocatalysts

TP@Y and TP@β were prepared starting from commercial NaY or H beta (P.Q. Industries), respectively, following the reported procedure.[3] To prepare TPTP@zeolite, a solution of chalcone (21 mg) and acetophenone (12 mg) in cyclohexane (10 ml) saturated with H_2S was stirred magnetically in the presence of thermally dehydrated (500 °C) HY or Hβ zeolites at reflux temperature for three days while a continuous stream of H_2S was passed through the system. Saturation of the whole system (solvent, zeolite and flask) with H_2S is crutical in order to minimize the concomitant formation of TP^+. In cases where a continuous flow of H_2S through the system was not maintained, IR spectra showed an enhancement of the 1623 cm^{-1} peak due to TPTP with respect to that presented in Fig. 3. During the ship-in-a-bottle synthesis, the solids become increasingly orange in color. When the reaction was complete, the raw TPTP@zeolite solids were subjected to exhaustive solid–liquid extraction using a Soxhlet apparatus and dichloromethane as solvent. TPTP@Y and TPTP@β were characterized by

combustion chemical analysis (Fisons CHNS analyzer) and spectroscopic techniques. Diffuse reflectance UV-Vis spectra were recorded on a Cary 5G spectrophotometer equipped with an integrating sphere and using $BaSO_4$ as the standard. FT-IR spectra were obtained with a Nicolet 710 spectrophotometer using sealed greaseless CaF_2 cells. Self-supporting wafers (10 mg) were prepared by pressing the powders at 2–3 ton cm^{-2} for 1 min. The IR spectra were recorded at room temperature after outgassing the samples at 200 °C and 10^{-2} Pa for 1 h.

Photophysical measurements

The emission spectrum of TPTP@Y was recorded on a Edinburgh FL900 spectrophotometer equipped with a Cerny monochromator and using a doped Xenon lamp with a front-face attachment. The measurements were made a room temperature by placing the powder in a 3 × 7 mm quartz cell capped with a septum. The solid was purged with nitrogen for at least 15 min before recording the spectrum. Laser flash photolysis was carried out using the third harmonic of a Spectron Nd:YAG laser system (15 mJ $pulse^{-1}$, <10 ns), using a 125 W Xenon lamp as the monitoring light. The diffuse reflectance from the excited solid surface was collected by fiber optics and transferred to a grating monochromator focused on a 9 dynodes photomultiplier. The powders were placed in 3 × 7 mm quartz cells and capped with septa. The samples were purged with N_2 or O_2 for at least 15 min before the experiment.

Photocatalytic activity

Tests were carried out using aqueous solutions of phenol (Aldrich, 40 ppm) or aniline (Aldrich, 40 ppm) in milliQ water (20 ml). In the aniline solution, the pH was set to 3 using dilute H_2SO_4. To these solutions, the corresponding weight of photocatalyst (30 mg for a typical experiment) was added and the suspension stirred magnetically. Irradiations were carried out using a 125 W medium pressure Hg lamp cooled by water through Pyrex. Test tubes containing the samples were placed surrounding the lamp well and independent tubes were used for each data point. At the required reaction time, the corresponding test tube was taken and the suspension was centrifuged. The solid was sonicated in an ultrasound bath (25 W) for 10 min after addition 3 ml milliQ water. After this time, the suspension was centrifuged and the extract combined with the photolyzed solution. Quantification of the phenol and aniline present in the combined aqueous solution was accomplished by quantitative HPLC using a reverse-phase column and a CH_3CN–H_2O (36 : 64) mixture as eluent. The concentration of phenol and aniline in the solutions was determined by integration of the chromatographic peak from a diode-array UV-Vis detector using 280 nm as the monitoring wavelength. A control experiment (40 ppm phenol, 30 mg TPTP@Y, 10^{-3} M H_2O_2) was carried out, wherein the percentage of phenol was measured at different times (up to 4 h) after switching off the lamp. The results showed that the phenol concentration remained constant in this time interval, independent of the time elapsed between the photochemical reaction and the HPLC quantification.

Acknowledgement

Financial support by the Spanish DGES through a grant (MAT 2000-1768-CO2-01) and a Fellowship to M. N. (SB99-BR0167839) is gratefully acknowledged.

References

1 M. A. Miranda and H. García, 2,4,6-Triphenylpyrylium tetrafluoroborate as an electron-transfer photosensitizer, *Chem. Rev.*, 1994, **94**, 1063.
2 A. Sanjuan, M. Alvaro, A. Corma and H. García, An organic sensitizer within Ti-zeolites as photocatalyst for the selective oxidation of olefins using oxygen and water as reagents, *Chem. Commun.*, 1999, 1641.
3 A. Corma, V. Fornés, H. García, M. A. Miranda, J. Primo and M. J. Sabater, Photoinduced electron transfer within zeolite cavities: cis-stilbene isomerization photosensitized by 2,4,6-triphenylpyrylium cation imprisoned inside zeolite Y, *J. Am. Chem. Soc.*, 1994, **116**, 2276.
4 A. Sanjuan, G. Aguirre, M. Alvaro and H. García, 2,4,6-Triphenylpyrylium ion encapsulated in Y zeolite as photocatalyst. A cooperative contribution of the zeolite host to the photodegradation of 4-chlorophenoxyacetic acid using solar light, *Appl. Catal., B*, 1998, **15**, 247.
5 A. Sanjuan, G. Aguirre, M. Alvaro, H. García and J. C. Scaiano, Degradation of propoxur in water using 2,4,6-triphenylpyrylium-Zeolite Y as photocatalyst. Product study and laser flash photolysis, *Appl. Catal., B*, 2000, **25**, 257.
6 O. Legrini, E. Oliveros and A. Braun, Photochemical processes for water treatment, *Chem. Rev.*, 1993, **93**, 671.
7 A. T. Balaban, A. Dinculescu, G. N. Dorofeenko, G. V. Fisher, A. V. Kablik, V. V. Mezheritskii and W. Schroth, Pyrylium salts: synthesis, reactions, and physical properties, *Adv. Heterocycl. Chem., Suppl. Vol. 2*, 1982.
8 N. Manoj, A. Kumar and K. R. Gopidas, Photophysical and electron transfer studies of a few 2,6-dimethyl-4-(alkylphenyl)-pyrylium and thiopyrylium derivatives, *J. Photochem. Photobiol., A*, 1997, **109**, 109.
9 S. S. Jayanthi and P. Ramamurthy, Excited singlet state reactions of thiopyrylium with electron donors: electron transfer, induction of triplet by internal and external heavy atom effect and comparison of pyrylium and thiopyrylium reactions, *J. Phys. Chem. A*, 1998, **102**, 511.
10 A. Sanjuan, M. Alvaro, G. Aguirre, H. García and J. C. Scaiano, Intrazeolite photochemistry. 21. 2,4,6-Triphenylpyrylium encapsulated inside zeolite Y supercages as heterogeneous photocatalyst for the generation of hydroxyl radical, *J. Am. Chem. Soc.*, 1998, **120**, 7351.
11 G. Meyer, D. Woehrle, M. Molh and G. Schulz-Elkloff, Synthesis of faujasite supported phthalocyanines of cobalt, nickel and copper, *Zeolites*, 1984, **4**, 30.
12 N. Herron, G. D. Stucky and C. A. Tolman, Shape selectivity in hydrocarbon oxidations using zeolite-encapsulated iron phthalocyanine catalysts, *J. Chem. Soc.*, 1986, **20**, 1521.
13 W. H. Quayle, J. H. Lunsford, G. Peeters, G. L. De Roy and E. F. Vansant, Synthesis and spectroscopic properties of divalent and trivalent tris(2,2′-dipyridine)iron complexes in zeolite Y, *Inorg. Chem.*, 1982, **21**, 2226.
14 J. C. Scaiano and H. Garcia, Intrazeolite photochemistry: toward supramolecular control of molecular photochemistry, *Acc. Chem. Res.*, 1999, **32**, 783.
15 M. L. Cano, F. L. Cozens, H. García, V. Marti and J. C. Scaiano, Intrazeolite photochemistry. 13. Photophysical properties of bulky 2,4,6-triphenylpyrylium and tritylium cations within large- and extra-large-pore zeolites, *J. Phys. Chem.*, 1996, **100**, 18 152.
16 F. D. Saeva and G. R. Ollin, Electron-donating properties of oxygen vs. sulfur. Redox potentials for some pyrylium and thiapyrylium salts, *J. Am. Chem. Soc*, 1980, **102**, 299.
17 S. H. Bossmann, D. Herrmann, A. M. Braun and C. Turro, Ruthenium (II)-tris-bipyridine/TiO_2/platinum-doped zeolite Y photocatalysts: photochemical generation of hydrogen (H_2) and oxidation of 2,4-dimethylaniline, *J. Inf. Rec.*, 1998, **24**, 271.
18 T. O. Zhang, T. Aoshima, A. Hidaka, H. Zhao and J. Serpone, Photooxidative N-demethylation of methylene blue in aqueous TiO_2 dispersions under UV irradiation, *J. Photochem. Photobiol., A*, 2001, **140**, 163.
19 S. Bossmann, C. Turro, C. Schnabel, M. R. Pokhrel, L. M. J. Payawan, B. Baumeister and M. Woerner, $Ru(bpy)_3^{2+}$/TiO_2-codoped zeolites: synthesis, characterization, and the role of TiO_2 in electron transfer, *J. Phys. Chem. B*, 2001, **105**, 5374.
20 S. Bossmann, N. Shahin, L. Thanh, A. Bonfill, M. Worner and A. Braun, $[Feii(bpy)_3]^{2+}$/TiO_2-codoped zeolites: synthesis, characterization, and first application in photocatalysis, *Chem. Phys. Chem.*, 2002, **3**, 401.
21 D. Rehm and A. Weller, Kinetics and mechanism of electron transfer in fluorescence quenching in acetonitrile, *Ber. Bunsen-Ges. Phys. Chem.*, 1969, **73**, 834.